Sphingosine-1-phosphate receptor type 2 ($S1P_2$) inhibits bleomycin-induced cellular senescence in murine lung fibroblasts

Department of Molecular Vascular Physiology, Kanazawa University
Juanjuan Zhao, Yasuo Okamoto, Yoh Takuwa

Abstract

The lysophospholipid mediator sphingosine-1-phosphate (S1P) exerts diverse biological activities including the regulation of leukocyte migration and vascular barrier integrity, suggesting that S1P signaling could be involved in inflammatory fibrotic diseases. Pulmonary fibrosis is a devastating disease characterized by fibroblast accumulation and extracellular matrix deposition in lungs, and bleomycin–induced pulmonary fibrosis is the most widely used experimental model. We studied the effects of the S1P–specific receptor $S1P_2$ on the phenotypes of lung fibroblasts isolated from bleomycin- and saline-administered wild-type and $S1P_2$–null (*S1pr2*$^{-/-}$) mice. The lung fibroblasts from bleomycin-administered wild-type and *S1pr2*$^{-/-}$ mice failed to proliferate in the presence of serum, unlike fibroblasts from saline-administered mice. The fibroblasts from bleomycin-administered mice also showed the enlarged and flattened morphology compared with fibroblasts from control mice. Bleomycin administration increased the protein expression of the cell cycle inhibitor $p16^{INK4a}$ in fibroblasts and the number of senescence–associated β-galactosidase (SA-β-gal)-positive fibroblasts. In *S1pr2*$^{-/-}$ fibroblasts, bleomycin administration-induced increases in $p16^{INK4a}$ protein expression and SA–β-gal–positive cells were augmented. Furthermore, bleomycin increased mRNA expression of interleukin-6 and matrix metalloproteinases in *S1pr2*$^{-/-}$ fibroblasts compared with wild-type fibroblasts. In addition, the activation of Akt in response to platelet–derived growth factor and S1P was enhanced in *S1pr2*$^{-/-}$ fibroblasts compared with wild-type fibroblasts. These results indicate that $S1P_2$ deletion enhances bleomycin administration–induced cellular senescence of lung fibroblasts, which may lead to inhibition of lung fibrosis through the mechanisms involving increased matrix metalloproteinases expression. Thus, $S1P_2$ may be a novel therapeutic target for lung fibrosis.

Key word: fibroblasts, bleomycin, fibrosis, cellular senescence, sphingosine-1-phosphate, $S1P_2$

Introduction

Idiopathic pulmonary fibrosis (IPF) is a chronic and ultimately fatal disease characterized by scarring and chronic pathological remodeling of the lung in which the normal tissue architecture is progressively replaced by extracellular matrix (ECM) proteins including collagens and fibronectin, eventually leading to respiratory failure[1)2)]. Pulmonary fibrosis is also caused by collagen diseases, viral infections,

平成28年2月5日受付，平成28年2月29日受理

Abbreviations: BSA, bovine serum albumin; Ct, threshold cycle; DMEM, Dulbecco's modified Eagle's medium; cDNA, complementary DNA; ECM, extracellular cellular matrix; EC, endothelial cell; FBS, fetal bovine serum; GAPDH, glyceraldehyde 3-phosphate dehydrogenase; IgG, immunoglobulin G; IL, interleukin; IPF, idiopathic pulmonary fibrosis; MMP, matrix metalloproteinase; p-Akt; Ser^{473}-phosphorylated–Akt; p-ERK, Thr^{202}, Tyr^{204}-phosphorylated–extracellular signal-related kinase; PI, phosphatidylinositol; PDGF, platelet–derived growth factor; PTEN, phosphatase and tensin homolog deleted on chromosome 10; p-p53, Ser^{15}-phosphorylated–p53; qPCR quantitative polymerase chain reaction; ROS, reactive oxygen species; SA–β-gal, senescence–associated β-galactosidase; αSMA, α-smooth muscle actin; S1P, sphingosine-1-phosphate; *S1pr2*$^{-/-}$, $S1P_2$–null; SphK, sphingosine kinase; TGF, transforming growth factor; WT, wild-type

anti-cancer agents, radiotherapy and aerosolized environmental toxins[1]. As experimental models of pulmonary fibrosis, administration of the anticancer drug bleomycin into mice and rats is commonly employed[1)2)]. Pulmonary fibrosis is likely elicited by persistent injury of alveolar epithelial and vascular endothelial cells (ECs), which induces the infiltration of leukocytes into injured sites. These damaged cells and infiltrated leukocytes release inflammatory cytokines and profibrogenic factors such as interleukin (IL)-6, IL-1β, tumor necrosis factor-α, and transforming growth factor-β (TGFβ)[1)2)]. The cytokines and profibrogenic factors activate resident fibroblasts to induce differentiation into myofibroblasts[1)-3)]. Myofibroblasts migrate and accumulate with the excessive synthesis and deposition of ECM to form fibrotic lesions[1)-3)]. In addition, bone marrow-derived circulating fibrocytes and epithelial cells- and EC-derived fibroblasts may also contribute to myofibroblasts in fibrotic lesions[3)].

Sphingosine-1-phosphate (S1P) is a pleiotropic lysophospholipid mediator and regulates various biological processes such as embryonic development, angiogenesis, vascular permeability and lymphocyte trafficking[4)-9)]. S1P is generated intracellularly by the phosphorylation of sphingosine, which is derived from the membrane sphingolipids including sphingomyelin and glycosphingolipids, by sphingosine kinases 1 and 2 (SphK1 and SphK2)[4)-9)]. Erythrocytes and vascular ECs export intracellular S1P into the plasma through membrane transporters including Spns2, contributing to a high (~1 μM) S1P concentration in plasma. In contrast, the S1P concentration in the interstitial fluid is estimated to be very low (several nM). S1P binds to five S1P-specific G protein-coupled receptors ($S1P_1$-$S1P_5$) to mediate many of these S1P actions by stimulating distinct but overlapping signaling pathways in a receptor subtype-specific manner[4)-9)]. For example, $S1P_1$ exclusively couples to G_i and activates phosphatidylinositol (PI) 3-kinase-Akt/Rac and Ras-ERK with stimulation of chemotaxis and cell proliferation, whereas $S1P_2$ predominantly couples to $G_{12/13}$ and activates Rho, leading to inhibition of Rac and Akt with suppression of cell migration and proliferation[4)-6)].

S1P regulates migration, proliferation and differentiation into myofibroblasts of fibroblasts[7]. Fibroblasts mainly express $S1P_1$, $S1P_2$, and $S1P_3$[10]. S1P increased expression of the myofibroblast marker α-smooth muscle actin (αSMA) and collagen synthesis in fibroblasts[11)12)]. Interestingly, the powerful profibrotic cytokine TGFβ stimulated expression of αSMA and SphK1, a synthesizing enzyme of S1P, in fibroblasts and knockdown of either SphK1, $S1P_2$ or $S1P_3$ inhibited TGFβ-induced myofibroblast differentiation, suggesting that SphK1-S1P-$S1P_2$/$S1P_3$ pathway participates in profibrotic actions of TGFβ[10]. Moreover, S1P concentrations in serum and bronchoalveolar lavage fluid in patients with IPF were elevated with increased expression of SphK1 in the lung tissue[13]. SphK1 expression was also increased in bleomycin-induced lung fibrotic regions in mice[10]. Intriguingly, genetic deletion of SphK1 attenuated bleomycin-induced lung fibrosis[14]. These observations implicated S1P in the pathogenesis of lung fibrosis[7]. Recently we have observed that $S1P_2$ deficiency reduced bleomycin-induced lung fibrosis in mice compared with wild-type (WT) mice (unpublished observation; Zhao J, Okamoto Y and Takuwa Y). However, the profibrotic role of $S1P_2$ on lung fibrosis remains unknown.

In this study, we investigated a role of $S1P_2$ in fibroblasts isolated from fibrotic lungs of bleomycin-administered mice, by analyzing and comparing WT and $S1P_2$-null (*S1pr2*$^{-/-}$) lung fibroblasts. $S1P_2$ deletion dramatically enhanced bleomycin-provoked cellular senescence in lung fibroblasts; augmented cellular senescence in $S1P_2$-deficient fibroblasts was associated with suppressed cell proliferation and the upregulation of the cell cycle inhibitor protein $p16^{INK4a}$, senescence-associated β-galactosidase (SA-β-gal), and matrix metalloproteinases (MMPs) that degrade ECM proteins. The expression of cellular senescent phenotypes in lung fibroblasts of $S1P_2$-null mice may affect the development of bleomycin-induced lung fibrosis.

Materials and Methods

Materials

High-Capacity cDNA Reverse Transcription kit was purchased from Applied Biosystems (Foster, CA). S1P was bought from Biomol (Plymouth Meeting, PA). Rabbit polyclonal anti-$p16^{INK4a}$ antibody (sc-1207) was bought from Santa Cruz Biotechnology, Inc (Santa Cruz, CA). Rabbit polyclonal anti-Ser^{473}-phosphorylated Akt (p-Akt) antibody (#4060), rabbit polyclonal anti-Thr^{202}, Tyr^{204}-phosphorylated extracellular signal-related kinase (p-ERK) antibody (#4370), rabbit polyclonal

anti-Akt antibody (#9272), rabbit polyclonal anti-ERK antibody (#9102), rabbit polyclonal anti-Ser[15]-phosphorylated–p53 antibody (p–p53) (#9284), mouse monoclonal anti-p53 antibody (#2524), rabbit monoclonal anti-glyceraldehyde 3-phosphate dehydrogenase (GAPDH) antibody (#2118), anti-rabbit immunoglobulin G (IgG) alkaline phosphatase-conjugated secondary antibody (#7054), anti-mouse IgG alkaline phosphatase-conjugated secondary antibody (#7056) were bought from Cell Signaling Technology (Beverly, MA). Fetal bovine serum (FBS) was bought from Gibco Life technologies (Carlsbad, CA). Alamar Blue dye and TRIzol® were purchased from Invitrogen (Frederick, MD). Sodium pentobarbital was purchased from Kyoritsu (Tokyo, Japan). Bleomycin was bought from Nippon Kayaku (Tokyo, Japan). Platelet-derived growth factor-BB (PDGF-BB) was bought from Peprotech (Rocky Hill, NJ). Collagenase A and FastStart Universal SYBR Green Master were bought from Roche (Nutley, NJ). DNase I and fatty acid-free bovine serum albumin (BSA) were bought from Sigma (St. Louis, MO). Diff-Quik kit was bought from Sysmex (Kobe, Japan). Nuclear Fast Red (H-3403) was bought from Vector Laboratories (Burlingame, CA). 5-bromo-4-chloro-3-indolyl-β-D-galactopyranoside, 5-bromo-4-chloro-3-indolyl-phosphate, nitroblue tetrazolium, RPMI1640 and Dulbecco's modified Eagle's medium (DMEM) were bought from Wako Pure Chemical Co. (Osaka, Japan). All other reagents used were obtained from Wako Pure Chemical Co., unless otherwise specified.

Mice

$S1P_2$-null (*S1pr2*$^{-/-}$) mice were previously described[15]. *S1pr2*$^{-/-}$ mice (129Ola; C57BL/6J mixed background) were back-crossed with C57BL/6J mice (no. 000664; Charles River, Wilmington, Mass) once[15]. All mice were housed in a temperature-controlled environment (24℃) under a 12/12-hr light/dark cycle with regular chow and water *ad libitum*. All animal experiments were carried out in accordance with the Fundamental Guidelines for Proper Conduct of Animal Experiment and Related Activities in Academic Research Institutions under the jurisdiction of the Ministry of Education, Culture, Sports, Science and Technology of Japan, and were reviewed and approved by the Committee on Animal Experimentation and recombinant DNA experimentation of Kanazawa University. Mice were genotyped by PCR analysis of genomic DNA prepared from tail biopsies using the following primers[15]: F1, 5'-cagtgacaaaagctgccgaatgctgatgct-3'; F2, 5'-tggctacccgtgatattgctgaagagcttg-3'; R1, 5'-tgag cagtgagttaagggtggcaaaggcaa-3'. The PCR conditions were: 40 cycles of 94℃ (30 sec), 59℃ (45 sec) and 72℃ (30 sec) for F1 and R1, and 40 cycles of 94℃ (30 sec), 59℃ (45 sec) and 72℃ (30 sec) for F2 and R1. The amplified products were 424-bp in the wild-type allele and 241-bp in the targeted allele.

Bleomycin administration

WT and *S1pr2*$^{-/-}$ mice (8-10 week old, 20-25 g body weight) were injected intraperitoneally with bleomycin (0.035 μg/g body weight) or saline (150 μl)[16]. Mice were given bleomycin twice weekly for 4 weeks and sacrificed on day 22 and 33.

Isolation and culture of primary mouse lung fibroblasts

Primary mouse lung fibroblasts were isolated from lung tissues of bleomycin– or saline–administered mice by a previously described method[10]. Briefly, mouse lungs were cut into small pieces, minced, and digested enzymatically by collagenase A (1 mg/ml) and DNase I (50 U/ml) in DMEM supplemented with 10% FBS for 90 minutes. After filtration, released cells were centrifuged, washed, and cultured in DMEM supplemented with 10% FBS. The cells were passaged 2 times to obtain pure fibroblasts. The fibroblasts between passage 3 and 6 were used in this study.

Cell proliferation assay

Alamar Blue fluorescence assay was performed according to the manufacturer's instructions. Briefly, lung fibroblasts were plated in 96-well culture plates at a density of 1×10^3 cells per well in 100 μl of 10% FBS-containing DMEM in 5% CO_2 at 37 ℃ under humidified atmosphere for 24 hr. Then, after 24 hr of serum-free starvation, the cells were cultured in 2% FBS-containing DMEM for 4 days. Ten μl of Alamar blue dye was added daily to the appropriate wells and then incubated for 4 hr to allow proliferative cells to react with the reagent. The resulting fluorescent intensity (544 nm excitation/590 nm emission) was measured by a microplate fluorometer (Fluoroskan Ascent FL, Thermo Fisher Scientific Inc., Waltham, MA). The background values in the control wells containing only medium were subtracted. Prior to the treatment with 2% FBS, Alamar blue dye was added to fibroblasts and the fluorescent intensity at day 0 was recorded to confirm the similar basic levels in the groups.

Transwell migration assay

Transwell migration of lung fibroblasts was determined in a modified Boyden chamber (Neuro-Probe, Gaithersburg, MD) using polycarbonate filters with 8-μm pores as previously described[17]. Lung fibroblasts (2.5×10^5 cells) in 200 μl of serum-free RPMI1640 containing 0.1% fatty acid-free BSA was loaded into the upper wells, whereas the lower wells were filled with same medium containing various concentrations of S1P and/or PDGF (50 ng/ml). The cells were allowed to migrate across the porous filter for 6 hr at 37℃ in a CO_2 incubator. After staining with Diff-Quik and scraping the upper surface of the filter, the number of cells that migrated to the lower side of filter was determined by measuring optical densities at 595 nm using a 96-well microplate reader (Multiskan GO, Thermo Fisher Scientific Inc., Waltham, MA).

RNA isolation and real-time quantitative polymerase chain reaction (qPCR)

Total RNA was extracted from lung fibroblasts using TRIzol reagent according to the manufacturer's instruction. Two μg of total mRNA was reverse-transcribed into complementary DNA (cDNA) using a High-Capacity cDNA Reverse Transcription kit. Target gene expression was quantified with qPCR using FastStart Universal SYBR Green Master reagent and the ABI PRISM 7300 Sequence Detection system (Applied Biosystems, Foster City, CA). The condition for qPCR was 10 min at 95℃, followed by 40 cycles of 15 sec at 95℃ and 1 min at 60℃. The housekeeping gene β-actin was used as an internal control. To confirm the amplification specificity, PCR products from each primer part were subjected to a melting curve analysis and subsequent agarose gel electrophoresis. Primers, which were designed using Primer3Plus (http: //primer3plus.com/cgi-bin/dev/primer3plus.cgi) based on published sequence data from the Ensembl database (www.ensembl.org/Mus_musculus/), are listed in Table 1. An average threshold cycle (Ct) value was calculated from duplicate results for each gene and was normalized to that of β-actin to obtain the ΔCt value.

Western blotting analysis

Lung fibroblasts were treated as indicated and lysed in a cell lysis buffer containing 50 mM Tris-HCl (pH 7.4), 150 mM NaCl, 5 mM EDTA, 1% Triton X-100, 1 mM Na_3VO_4, 10 mM NaF, and 10 mM Na-β-glycerophosphate by scraping. The cell lysates were centrifuged at 15,000 rpm for 15 min at 4℃ and the resultant supernatants were separated by SDS-10% polyacrylamide gels, followed by electrotransfer onto Immobilon-P membrane (Millipore, Bedford, MA). The membranes were blocked with Tris-buffered saline (pH 7.4) containing 0.1% Tween-80 and 5% non-fat dry milk for 1 hr at room temperature and probed with rabbit polyclonal anti-Ser^{473}-p-Akt antibody (1: 1000 dilution), rabbit polyclonal anti-Thr^{202}, Tyr^{204}-p-ERK antibody (1: 1000), rabbit polyclonal anti-Akt antibody (1: 1000), rabbit polyclonal anti-ERK antibody (1: 1000), rabbit polyclonal anti-$p16^{INK4a}$ antibody (1: 500), mouse polyclonal anti-p53 antibody (1: 500), rabbit polyclonal anti-Ser^{15}-p–p53 antibody (1: 500) or rabbit monoclonal anti-GAPDH antibody (1: 1000). The bound antibodies were visualized using anti-rabbit or anti-mouse IgG alkaline phosphatase–conjugated secondary antibody (1: 1000) and 5-bromo-4-chloro-3-indolyl phosphate and nitro blue tetrazolium. Relative quantification of proteins was determined by scanning and band densitometry using Image Gauge software (Fuji Photo Film Co, Ltd, Tokyo, Japan).

SA-β-gal staining

SA-β-gal activity was performed as previously described with slight modifications[18]. Lung fibroblasts were washed twice with PBS and fixed in PBS containing 2% paraformaldehyde and 0.2% glutaraldehyde. Then, the cells were washed with PBS and incubated overnight at 37℃ with a freshly prepared SA-β-gal staining solution containing 1 mg/ml 5-bromo-4-chloro-3-indolyl-β-D-galactopyranoside, 40 mM citric acid-phosphate buffer (pH 6.0), 5 mM potassium ferrocyanide, 5 mM potassium ferricyanide, 2 mM $MgCl_2$ and 150 mM NaCl. The cells were counterstained with Nuclear Fast Red. The number of SA-β-gal-positive cells per total number of cells in the same field was determined by counting least 10 fields (x400) under bright-field microscope (BX 41; Olympus, Tokyo, Japan).

Statistical analysis

All values are expressed as means ± SEM. Statistical significance of differences were analyzed with Prism 6 software (GraphPad Software, San Diego, CA) using two-way ANOVA followed by Bonferroni post-test. $P < 0.05$ was considered to denote significance.

Results

Effects of $S1P_2$ deletion on cell proliferation and migration of lung fibroblasts from bleomycin-administered and non-administered mice

We followed cell proliferation of lung fibroblasts in the presence of 2% FBS for 4 days. The fibroblasts from saline-administered *S1pr2*$^{-/-}$ mice more robustly proliferated than the cells from saline-administered WT mice (Fig. 1). In contrast to fibroblasts from saline-administered mice, the fibroblasts from bleomycin-administered WT or *S1pr2*$^{-/-}$ mice did not proliferate in the presence of 2% FBS. The fibroblasts from bleomycin-administered WT and *S1pr2*$^{-/-}$ mice were enlarged and flattened compared with fibroblasts from saline-administered mice (data not shown).

We studied the effects of $S1P_2$ deficiency on cell migration of lung fibroblasts, using a transwell migration assay. PDGF directed chemotaxis in both WT and *S1pr2*$^{-/-}$ fibroblasts, whether they were derived from saline- or bleomycin-administered mice (Fig. 2 A and B). However, the migratory responses to PDGF were sluggish in lung fibroblasts from bleomycin-administered *S1pr2*$^{-/-}$ mice. S1P induced dose-dependent inhibition of PDGF-directed chemotaxis and random migration without PDGF in WT fibroblasts from saline- and bleomycin-administered mice. In contrast, S1P did not inhibit PDGF-directed chemotaxis or random migration in *S1pr2*$^{-/-}$ fibroblasts. Thus, $S1P_2$ mediated S1P-induced inhibition of cell migration in lung fibroblasts as previously observed in other types of cells including vascular smooth muscle cells and tumor cells[19)20)].

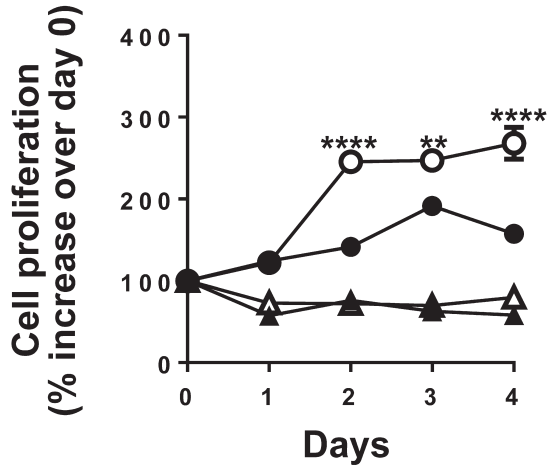

Fig. 1. Cell proliferation of lung fibroblasts isolated from WT and *S1pr2*$^{-/-}$ mice with bleomycin or saline administration.
The lung fibroblasts isolated from WT and *S1pr2*$^{-/-}$ mice on day 33 after starting administration of bleomycin or saline were serum-starved for 24 hr and the proliferation of cells in the presence of 2% FBS was determined using Alamar Blue assay. Data are shown the means ± SEM (n=8) and are representative of three independent experiments. The closed and open circles / triangles represent lung fibroblasts from WT and *S1pr2*$^{-/-}$ mice, respectively. The circles and triangles represent fibroblasts from saline– and bleomycin–administered mice, respectively. The values at day 0 were expressed as 100%. The symbols ** and **** denote statistical significance at the levels of P<0.01 and P<0.0001, respectively, compared with the values of fibroblasts from saline-administered WT mice.

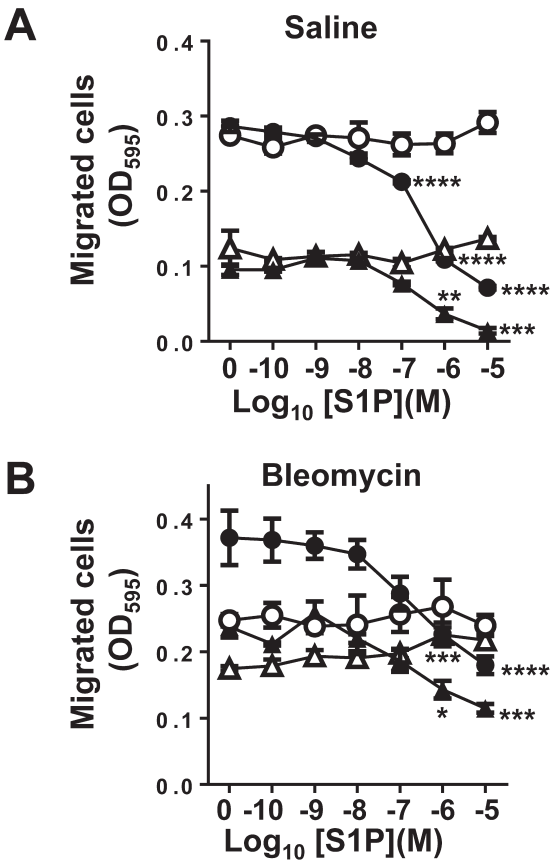

Fig. 2. Migration of lung fibroblasts isolated from WT and *S1pr2*$^{-/-}$ mice with or without bleomycin challenge.
Transwell migration of lung fibroblasts from saline-administered mice (A) and bleomycin-administrated mice (B) was determined in the presence of various concentrations of S1P and/or PDGF-BB (50 ng/ml) placed in the lower well of the Boyden chamber. The closed and open circles/triangles represent lung fibroblasts from WT and *S1pr2*$^{-/-}$ mice, respectively. The circles and triangles represent PDGF-directed chemotaxis and random migration, respectively. OD indicates optical density. Data are means ± SEM from three independent experiments, each performed in duplicates. The symbols *, **, *** and **** denote statistical significance at the levels of P<0.05, P<0.01, P<0.001 and P<0.0001, compared with the values in the cells without S1P treatment in the same group.

Effects of $S1P_2$ deletion on mRNA expression of inflammatory and profibrotic cytokines in lung fibroblasts

It has been reported that activated fibroblasts in fibrotic lesions produce and secrete inflammatory cytokines and profibrotic mediators to further promote inflammation and activation of fibroblasts [1)3)]. The mRNA expression of IL-6, IL-1β or TGFβ1 was not altered in lung fibroblasts isolated from WT mice that received bleomycin (Table 2). In *S1pr2*$^{-/-}$ lung fibroblasts, bleomycin administration increased mRNA expression of IL-6 but not IL-1β or TGFβ1. IL-6 mRNA level in lung fibroblasts from bleomycin-administered *S1pr2*$^{-/-}$ mice was higher compared with the WT counterpart.

Effects of $S1P_2$ deficiency on bleomycin-induced $p16^{INK4a}$ expression and SA-β-gal activity in lung fibroblasts

The fibroblasts from bleomycin-administered mice exhibited suppression of cell proliferation, morphological changes, and upregulation of IL-6 expression compared with control fibroblasts (Fig.1 and Table 2), raising the possibility that they might be senescent[21)]. We tested this possibility by examining expression of the cellular senescence markers $p16^{INK4a}$ and SA-β-gal activity in lung fibroblasts. Bleomycin administration increased the protein expression of the cell cycle inhibitor $p16^{INK4a}$ in fibroblasts isolated from either WT or *S1pr2*$^{-/-}$ mice (Fig. 3A). The expression of $p16^{INK4a}$ in *S1pr2*$^{-/-}$ fibroblasts from bleomycin-administered mice was higher compared with the WT counterpart. We also examined another cellular senescence marker p53 protein and Ser^{18} phosphorylation of p53 (corresponding to Ser^{15} in human p53), which is induced by DNA damage, in lung fibroblasts[22)]. Bleomycin administration did not increase p53 protein or p-p53 in WT or *S1pr2*$^{-/-}$ fibroblasts (Fig. 3B). SA-β-gal–positive cells were negligible in both WT and *S1pr2*$^{-/-}$ lung fibroblasts from saline-administered mice whereas SA-β-gal–positive cells were increased in fibroblasts from bleomycin-administered WT mice (Fig. 4). SA-β-gal-positive cells were further increased in fibroblasts from bleomycin-administered *S1pr2*$^{-/-}$ mice. These results together indicated that bleomycin administration induced cellular senescence of lung fibroblasts, which was enhanced by $S1P_2$ deletion.

Table 1. Primer pairs used in qPCR

Genes	Primer pair sequences (forward/reverse)
IL-6	5'-ccggagaggagacttcacag-3' 5'-tccacgatttcccagagaac-3'
IL-1β	5'-caggcaggcagtatcactca-3' 5'-aggccacaggtattttgtcg-3'
TGFβ1	5'-tgcgcttgcagagattaaaa-3' 5'-cgtcaaaagacagccactca-3'
MMP1	5'-aactacatttaggggagaggtgt-3' 5'-gcagcgtcaagtttaactggaa-3'
MMP2	5'-caagttccccggcgatgtc-3' 5'-ttctggtcaaggtcacctgtc-3'
MMP3	5'-actctaccactcagccaagg-3' 5'-tccagagagttagacttggtgg-3'
MMP9	5'-ctggacagccagacactaaag-3' 5'-ctcgcggcaagtcttcagag-3'
Fibronectin	5'-tctgggaaatggaaaaggggaatgg-3' 5'-cactgaagcaggtttcctcggttgt-3'
Collagen type 1α1	5'-cctggcaaagacggactcaac-3' 5'-gctgaagtcataaccgccactg-3'
β-actin	5'-aggtcatcactattggcaacga-3' 5'-cacttcatgatggaattgaatgtagtt-3'

IL, interleukin; MMP, matrix metalloproteinase

Table 2. Messenger RNA expression of inflammatory cytokines, matrix metalloproteinases and extracellular matrix proteins in lung fibroblasts from WT and *S1pr2*$^{-/-}$ mice with and without bleomycin administration

	WT		*S1pr2*$^{-/-}$	
Genes	Saline	Bleomycin	Saline	Bleomycin
IL-6	8.00 ± 0.45	8.00 ± 0.44	5.97 ± 0.16	11.3 ± 0.71 *** ,##
IL-1β	4.02 ± 1.72	6.85 ± 2.24	5.11 ± 2.17	6.99 ± 2.73
TGFβ1	3.62 ± 0.16	4.46 ± 0.43	3.52 ± 0.34	3.99 ± 0.51
MMP1	1.13 ± 0.14	3.10 ± 0.94	1.11 ± 0.20	30.2 ± 3.56 *** ,###
MMP2	3.52 ± 0.48	4.89 ± 0.59	4.58 ± 0.31	81.1 ± 12.4 *** ,###
MMP3	5.03 ± 0.29	8.55 ± 0.55	3.87 ± 0.19	46.0 ± 3.94 *** ,###
MMP9	4.89 ± 0.78	3.57 ± 0.66	3.73 ± 0.57	5.49 ± 0.31 * ,#
Collagen Iα1	1.70 ± 0.09	1.95 ± 0.13	1.87 ± 0.29	2.34 ± 0.17
Fibronectin	1.65 ± 0.13	1.71 ± 0.28	1.36 ± 0.17	1.41 ± 0.46

Messenger RNA levels in lung fibroblasts isolated on day 33 after starting administration of saline or bleomycin were determined with qPCR. The values shown were obtained by multiplying ΔCt values ((Ct of gene of interest) - (Ct of β-actin)) by 10^{-3} for IL-6, TGFβ1, MMP2 and MMP3, by 10^{-7} for IL-1β, by 10^{-6} for MMP1, by 10^{-5} for MMP9, and by 10^{-1} for collagen Iα1 and fibronectin. Data are means ± SEM from three independent experiments, each performed in duplicates. The symbols * and *** denote statistical significance at the level of $P<0.05$ and $P<0.001$, respectively, compared with lung fibroblasts isolated from saline-administered WT mice. The symbols #, ## and ### denote statistical significance at the level of $P<0.05$, $P<0.01$ and $P<0.001$, respectively, compared with lung fibroblasts isolated from bleomycin-administered WT mice.

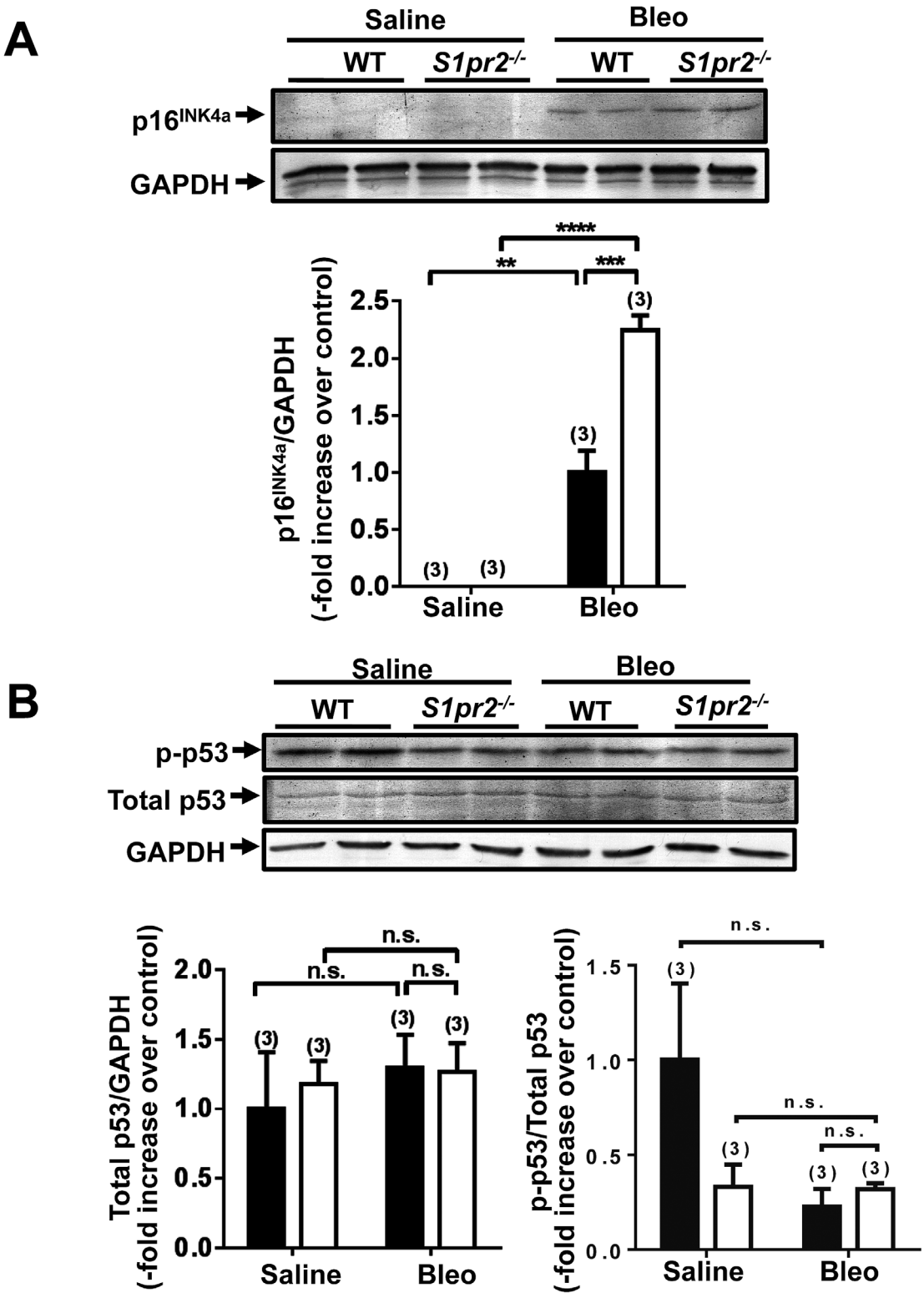

Fig. 3. Expression of $p16^{INK4a}$ and p53 proteins in lung fibroblasts isolated from WT and *S1pr2*$^{-/-}$ mice with bleomycin or saline administration.

Protein expression of $p16^{INK4a}$ (A), and total p53 and p-p53 (B) was determined with Western blotting in lung fibroblasts isolated from WT and *S1pr2*$^{-/-}$ mice on day 33 after starting administration of bleomycin or saline. In (A) and (B), GAPDH was used as an internal control. Top: representative blots. Bottom: quantified data. The bar graph represents the quantified data of $p16^{INK4a}$ and p-p53 proteins which were normalized to that of GAPDH and total p53, respectively, and expressed as fold-changes relative to the levels in fibroblasts from bleomycin-administered WT mice (A) or saline-administered WT mice (B). Data are means ± SEM from three independent experiments. The numbers in parentheses denote the analyzed data numbers throughout the Figures. The closed and open bars represent lung fibroblasts from WT and *S1pr2*$^{-/-}$ mice, respectively. The symbols denote the similar levels of statistical significance as described in Fig. 2. n.s.: not significant.

Effects of $S1P_2$ deletion on activation of Akt and ERK in lung fibroblasts

Because cellular senescence is known to be associated with stimulation of mitogenic signaling pathways including PI3K-Akt and Ras-ERK[23], we studied activation of Akt and ERK with Western blotting using anti-phospho-specific antibodies in lung fibroblasts isolated from bleomycin-administered mice. The baseline level of p-Akt was similar between WT and *S1pr2*$^{-/-}$ lung fibroblasts. In WT fibroblasts, the addition of S1P reduced the level of p-Akt whereas S1P tended to increase p-Akt in *S1pr2*$^{-/-}$ fibroblasts (Fig. 5A). This was probably because in WT fibroblasts $S1P_2$–mediated Akt inhibition predominated over $S1P_1$–mediated Akt phosphorylation whereas in *S1pr2*$^{-/-}$ fibroblasts S1P stimulated Akt phosphorylation via $S1P_1$. PDGF markedly increased p-Akt in both WT and *S1pr2*$^{-/-}$ lung fibroblasts. S1P tended to reduce PDGF-induced p-Akt increase in WT fibroblasts whereas S1P tended to enhance PDGF-induced increase in p-Akt in *S1pr2*$^{-/-}$ fibroblasts. In contrast to Akt, a change in ERK activation by PDGF or S1P was not detected (Fig. 5B). Thus, $S1P_2$ exerts an inhibitory effect on PDGF-induced Akt activation.

Effects of $S1P_2$ deletion on mRNA expression of MMPs and ECM proteins in lung fibroblasts

Because senescent cells are known to release the ECM-degrading enzymes MMPs more abundantly compared with non-senescent cells, we studied mRNA expression of MMPs and also ECM proteins in lung fibroblasts[22]. Administration of bleomycin into WT mice did not increase the mRNA expression of MMP1, MMP2, MMP3 or MMP9 in lung fibroblasts (Table 2). In contrast, bleomycin administration into *S1pr2*$^{-/-}$ mice markedly increased the mRNA expression of these MMPs. In WT or *S1pr2*$^{-/-}$ mice, bleomycin administration did not alter the mRNA expression of fibronectin or collagen Iα1 in lung fibroblasts. Also, there was no difference in the mRNA expression of fibronectin and collagen Iα1 between WT and *S1pr2*$^{-/-}$ fibroblasts.

Discussion

In this study, we demonstrate that administration of bleomycin into mice, which is widely employed as experimental animal model of lung fibrosis, induces cellular senescence of lung fibroblasts and that genetic deletion of $S1P_2$ augments bleomycin-induced senescence of lung fibroblasts. These

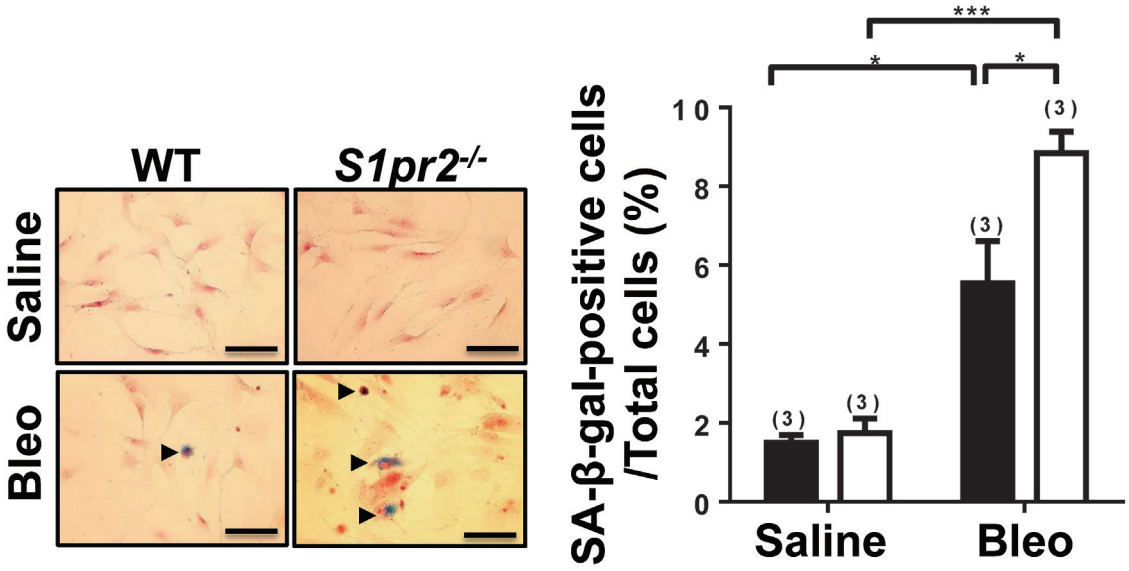

Fig. 4. SA-β-gal staining of lung fibroblasts isolated from WT and *S1pr2*$^{-/-}$ mice with bleomycin or saline administration.
The lung fibroblasts isolated from WT and *S1pr2*$^{-/-}$ mice on day 33 after starting administration of bleomycin or saline were stained for SA-β-gal activity. Left: representative photographs of SA-β-gal-positive cells counterstained with nuclear fast red (magnification x 400). Right: quantified data of SA-β-gal-positive cells. The cells stained in blue were counted as SA-β-gal-positive cells under a bright field microscope. Data are means ± SEM from three independent experiments. The numbers in parentheses denote the analyzed data numbers throughout the Figures. The closed and open bars represent lung fibroblasts from WT and *S1pr2*$^{-/-}$ mice, respectively. The symbols denote the similar levels of statistical significance as described in Fig. 2. Scale bar: 200 μm.

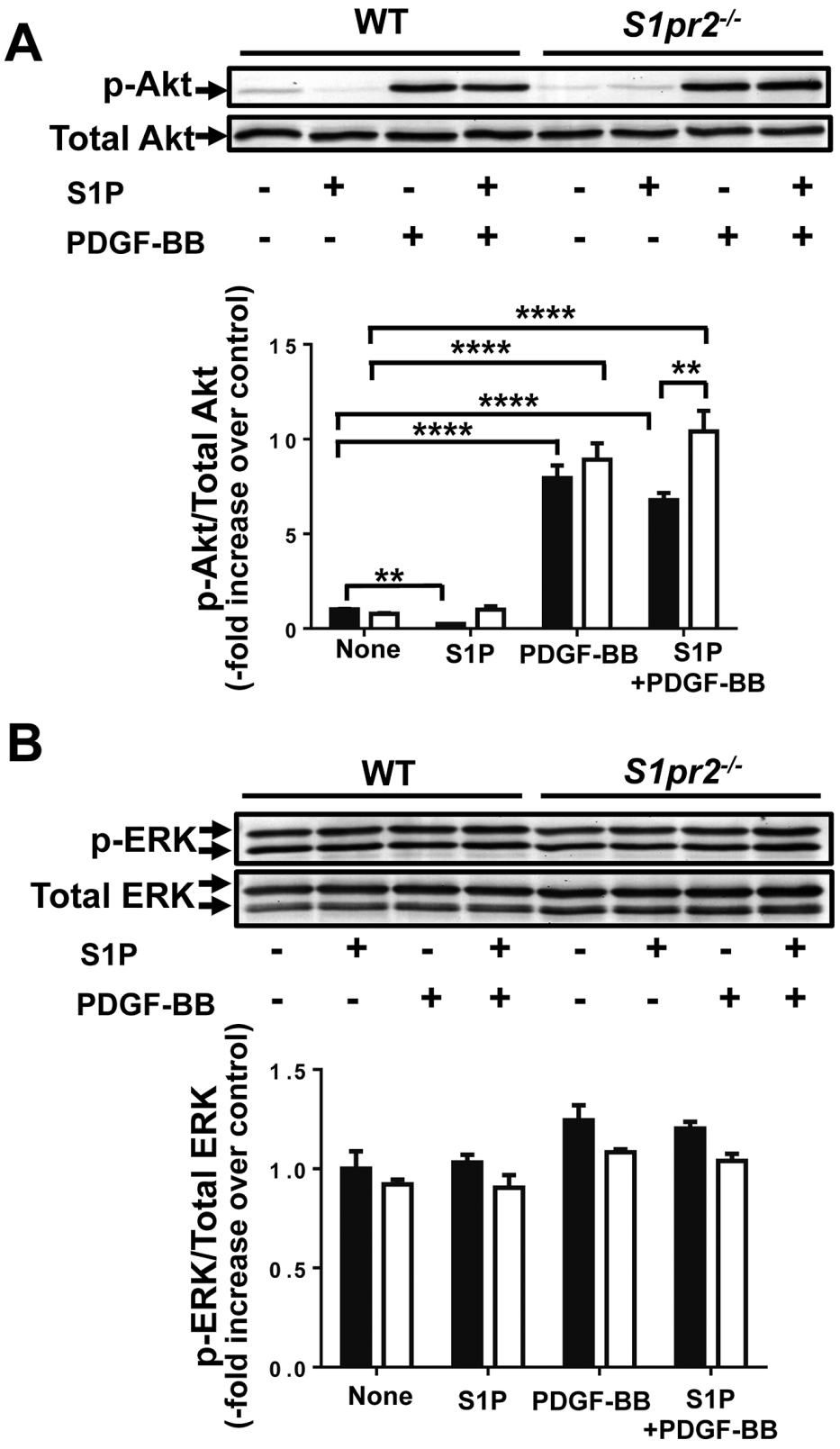

Fig. 5. Activation of Akt and ERK in lung fibroblasts isolated from WT and *S1pr2*$^{-/-}$ mice with bleomycin administration. Phosphorylation of Akt at Ser^{473} (A) and ERK at Thr^{202} and Tyr^{204} (B) was determined with Western blotting. The lung fibroblasts isolated from WT and *S1pr2*$^{-/-}$ mice on day 33 after starting bleomycin administration were serum-starved and treated with PDGF-BB (10 ng/ml) and/or S1P (0.3 μM) for 10 minutes. Top: representative blots. Bottom: quantified data. The bar graph shows the density of each band of phosphorylated proteins which was normalized to that of total proteins and expressed as fold-changes relative to the levels in non-treated fibroblasts. Data are means ± SEM from three independent experiments. The closed and open bars represent lung fibroblasts from WT and *S1pr2*$^{-/-}$ mice, respectively. The symbols denote the similar levels of statistical significance as described in Fig. 2.

findings may at least in part account for the lung phenotype of bleomycin-administered *S1pr2*$^{-/-}$ mice.

Cellular senescence is generally defined as the state where cells cannot divide any longer, as a result of the responses to a variety of cellular stresses including DNA damage, reactive oxygen species (ROS), and oncogene activation[21)-23)]. Senescent cells are characterized by irreversible growth arrest, enlarged nucleus and widely spread cellular morphology, increased SA-β-gal activity, and upregulation of the cell cycle inhibitors such as $p16^{INK4a}$ [21)22)]. Excessive release of a series of secreted proteins such as proinflammatory cytokines, chemokines and matrix-degrading enzymes, which is called senescence-associated secretory phenotype (SASP), is also a striking feature of cellular senescence[21)22)]. In the present study, the lung fibroblasts isolated from bleomycin-administered WT and *S1pr2*$^{-/-}$ mice showed markedly reduced proliferation, an enlarged and flattened morphology, increased $p16^{INK4a}$ expression and SA-β-gal activity, and enhanced expression of IL-6 and MMPs compared with the saline-administered counterparts (Figs. 1, 3 and 4 and Table 2), indicating that bleomycin administration induced cellular senescence in lung fibroblasts.

One of the major side effects of bleomycin, which is a chemotherapeutic agent to be commonly used for treating various types of cancer, is lung injury, particularly lung fibrosis[24)]. Bleomycin exerts cytotoxic effects by causing the cleavage of DNA strand, which involves the generation of ROS[24)]. In the lung, bleomycin damages pulmonary epithelial cells and other types of cells to release various substances, collectively called damage-associated molecular pattern[25)-27)]. These "danger signals" are suggested to directly and indirectly activate inflammatory cells, releasing profibrotic cytokines which include TGFβ[25)-27)]. ROS generated by the bleomycin action may also contribute to the development of cellular senescence of lung fibroblasts.

A recent study of liver fibrosis showed that entry of myofibroblasts into senescence induced irreversible proliferative arrest, inhibition of ECM accumulation and clearance of myofibroblasts by natural killer cells in fibrotic liver[28)]. In other studies, the ECM protein CCN1 was shown to promote fibroblasts senescence and the expression of MMPs, which helped to resolve fibrosis in the cutaneous wound healing and liver fibrosis models[29)30)]. Taken together, it is suggested that cellular senescence of fibroblasts may alleviate fibrosis during tissue repair processes in various tissues. Our observations suggest that cellular senescence of lung fibroblasts could contribute to the attenuation of fibrosis through the mechanisms involving reduced fibroblast proliferation and increased MMP expression. Notably, $S1P_2$ deficiency facilitated cellular senescence of lung fibroblasts, suggesting that $S1P_2$ deficiency may attenuate fibrosis. In fact, we recently found that *S1pr2*$^{-/-}$ mice given bleomycin showed attenuation of lung fibrosis compared with WT mice (unpublished observation; Zhao J, Okamoto Y and Takuwa Y). Thus, $S1P_2$ might positively regulate the fibrotic process through antagonizing progression of fibroblast senescence.

$S1P_2$ may regulate cellular senescence of fibroblasts through multiple mechanisms. The lung fibroblasts in *S1pr2*$^{-/-}$ mice may have been more severely exposed to bleomycin compared with WT mice. We previously demonstrated that $S1P_2$ in the vascular endothelium protects against vascular barrier disruption[31)32)]. We observed in *S1pr2*$^{-/-}$ mice that pulmonary vascular leakage at the initial stage after starting biweekly injection of bleomycin was more severe in *S1pr2*$^{-/-}$ mice than in WT mice (unpublished observation; Zhao J, Okamoto Y and Takuwa Y). Therefore, it is likely that fibroblasts in *S1pr2*$^{-/-}$ mice underwent accelerated cellular senescence through the enhanced direct toxic effects of bleomycin and indirect effects mediated by the generation of ROS. Alternatively, cellular senescence of *S1pr2*$^{-/-}$ fibroblasts may be promoted through the different regulation of "phosphatase and tensin homolog deleted on chromosome 10" (PTEN), which is a 3'-specific phosphoinositide phosphatase and converts PI-3,4,5-P_3 to PI-4,5-P_2. Loss of PTEN was shown to trigger cellular senescence[23)]. $S1P_2$ was previously demonstrated to stimulate PTEN[33)]. Consistent with this, WT fibroblasts showed an reduction in Akt phosphorylation in response to S1P stimulation whereas *S1pr2*$^{-/-}$ fibroblasts showed rather increased Akt phosphorylation in response to S1P (Fig. 5A). Therefore, de-inhibition of PTEN in *S1pr2*$^{-/-}$fibroblasts may also contribute to promotion of cellular senescence.

In summary, the present study demonstrates that the loss of $S1P_2$ in lung fibroblasts facilitates bleomycin-induced cellular senescence and, thereby,

may prohibit progression of lung fibrosis. These findings suggest that pharmacological blockade of $S1P_2$ may be a novel promising target for treating fibrotic disorders.

Acknowledgements

This work was supported by Grant-in Aids for Scientific Research from the Ministry of Education, Culture, Sports, Science, and Technology and a Grant-in Aid for Scientific Research on Innovative Areas from the Society for the Promotion of Science of Japan. We are grateful to Ms. Chiemi Hirose for her secretarial assistance.

References

1) Wynn TA. Integrating mechanisms of pulmonary fibrosis. J Exp Med 208: 1339-1350, 2011.

2) Wolters PJ, Collard HR, Jones KD. Pathogenesis of idiopathic pulmonary fibrosis. Annu Rev Pathol 9: 157-179, 2014

3) Kendall RT, Feghali-Bostwick CA. Fibroblasts in fibrosis: novel roles and mediators. Front Pharmacol 5: 123, 2014

4) Takuwa Y, Okamoto Y, Yoshioka K, Takuwa N. Sphingosine-1-phosphate signaling in physiology and diseases. Biofactors 38: 329-337, 2012

5) Takuwa Y, Okamoto Y, Yoshioka K, Takuwa N. Sphingosine-1-phosphate signaling and biological activities in the cardiovascular system. Biochim Biophys Acta 1781: 483-488, 2008

6) Takuwa Y. Subtype-specific differential regulation of Rho family G proteins and cell migration by the Edg family sphingosine-1-phosphate receptors. Biochim Biophys Acta 1582: 112-120, 2002

7) Takuwa Y, Ikeda H, Okamoto Y, Takuwa N, Yoshioka K. Sphingosine-1-phosphate as a mediator involved in development of fibrotic diseases. Biochim Biophys Acta 1831: 185-192, 2013

8) Takuwa N, Du W, Kaneko E, Okamoto Y, Yoshioka K, Takuwa Y. Tumor-suppressive sphingosine-1-phosphate receptor-2 counteracting tumor-promoting sphingosine-1-phosphate receptor-1 and sphingosine kinase 1 - Jekyll Hidden behind Hyde. Am J Cancer Res 1: 460-481, 2011.

9) Takuwa Y, Du W, Qi X, Okamoto Y, Takuwa N, Yoshioka K. Roles of sphingosine-1-phosphate signaling in angiogenesis. World J Biol Chem 1: 298-306, 2010

10) Kono Y, Nishiuma T, Nishimura Y, Kotani Y, Okada T, Nakamura S, Yokoyama M. Sphingosine kinase 1 regulates differentiation of human and mouse lung fibroblasts mediated by TGFβ1. Am J Respir Cell Mol Biol 37: 395-404, 2007

11) Urata Y, Nishimura Y, Hirase T, Yokoyama M. Sphingosine 1-phosphate induces alpha-smooth muscle actin expression in lung fibroblasts via Rho-kinase. Kobe J Med Sci 51: 17-27, 2005.

12) Keller CD, Rivera Gil P, Tölle M, van der Giet M, Chun J, Radeke HH, Schäfer-Korting M, Kleuser B. Immunomodulator FTY720 induces myofibroblast differentiation via the lysophospholipid receptor S1P3 and Smad3 signaling. Am J Pathol 170: 281-292, 2007

13) Milara J, Navarro R, Juan G, Peiró T, Serrano A, Ramón M, Morcillo E, Cortijo J. Sphingosine-1-phosphate is increased in patients with idiopathic pulmonary fibrosis and mediates epithelial to mesenchymal transition. Thorax 67: 147-156, 2012

14) Huang LS, Berdyshev E, Mathew B, Fu P, Gorshkova IA, He D, Ma W, Noth I, Ma SF, Pendyala S, Reddy SP, Zhou T, Zhang W, Garzon SA, Garcia JG, Natarajan V. Targeting sphingosine kinase 1 attenuates bleomycin-induced pulmonary fibrosis. FASEB J 27: 1749-1760, 2013

15) Du W, Takuwa N, Yoshioka K, Okamoto Y, Gonda K, Sugihara K, Fukamizu A, Asano M, Takuwa Y. S1P(2), the G protein-coupled receptor for sphingosine-1-phosphate, negatively regulates tumor angiogenesis and tumor growth in vivo in mice. Cancer Res 70: 772-781, 2010

16) Zhou Y, Schneider DJ, Morschl E, Song L, Pedroza M, Karmouty-Quintana H, Le T, Sun CX, Blackburn MR. Distinct roles for the A2B adenosine receptor in acute and chronic stages of bleomycin-induced lung injury. J Immunol 186: 1097-1106, 2011.

17) Okamoto H, Takuwa N, Yokomizo T, Sugimoto N, Sakurada S, Shigematsu H, Takuwa Y. Inhibitory regulation of Rac activation, membrane ruffling, and cell migration by the G protein-coupled sphingosine-1-phosphate receptor EDG5 but not EDG1 or EDG3. Mol Cell Biol 20: 9247-9261, 2000

18) Debacq-Chainiaux F, Erusalimsky JD, Campisi J, Toussaint O. Protocols to detect senescence-associated beta-galactosidase (SA-βgal) activity, a biomarker of senescent cells in culture and *in vivo*. Nat Protoc 4: 1798-1806, 2009.

19) Takashima S, Sugimoto N, Takuwa N, Okamoto Y, Yoshioka K, Takamura M, Takata S, Kaneko S, Takuwa Y. G12/13 and Gq mediate S1P2-induced inhibition of Rac and migration in vascular smooth muscle in a manner dependent on Rho but not Rho kinase. Cardiovasc Res 79: 689-697, 2008.

20) Arikawa K, Takuwa N, Yamaguchi H, Sugimoto N, Kitayama J, Nagawa H, Takehara K, Takuwa Y. Ligand-dependent inhibition of B16 melanoma cell migration and invasion via endogenous S1P2 G protein-coupled receptor . Requirement of inhibition of cellular RAC activity. J Biol Chem 278: 32841-32851, 2003.

21) Rodier F, Campisi J. Four faces of cellular senescence. J Cell Sci 192: 547-556, 2010.

22) Munoz-Espin D, Serrano M. Cellular senescence: from physiology to pathology. Nat Rev Mol Cell Biol 15: 482-496, 2014.

23) Xu Y, Li N, Xiang R, Sun P. Emerging roles of the p38 MAPK and PI3K/AKT/mTOR pathways in oncogene-induced senescence. Trends Biochem Sci 39: 268-276, 2014.

24) Della Latta V, Cecchettinin A, Del Ry S, Morales MA. Bleomycin in the setting of lung fibrosis induction: From biological mechanisms to counteractions. Pharmacol Res 97: 122-130, 2015

25) Kim HS, Go H, Akira S, Chung DH. TLR2-mediated production of IL-27 and chemokines by respiratory epithelial cells promotes bleomycin-induced pulmonary fibrosis in mice. J Immunol 187: 4007-4017, 2011

26) Luzina IG, Kopach P, Lockatell V, Kang PH, Nagarsekar A, Burke AP, Hasday JD, Todd NW, Atamas SP. Interleukin-33

potentiates bleomycin-induced lung injury. Am J Respir Cell Mol Biol 49: 999-1008, 2013

27) Suwara MI, Green NJ, Borthwick LA, Mann J, Mayer-Barber KD, Barron L, Corris PA, Farrow SN, Wynn TA, Fisher AJ, Mann DA. IL-1α released from damaged epithelial cells is sufficient and essential to trigger inflammatory resooponses in human lung fibroblasts. Mucosal Immunol 7: 684-693, 2014.

28) Krizhanovsky V, Yon M, Dickins RA, Hearn S, Simon J, Miething C, Yee H, Zender L, Lowe SW. Senescence of activated stellate cells limits liver fibrosis. Cell 134: 657-667, 2008

29) Jun JI, Lau LF. The matricellular protein CCN1 induces fibroblast senescence and restricts fibrosis in cutaneous wound healing. Nat Cell Biol 12: 676-685, 2010.

30) Kim KH, Chen CC, Monzon RI, Lau LF. Matricellular protein CCN1 promotes regression of liver fibrosis through induction of cellular senescence in hepatic myofibroblasts. Mol Cell Biol 33: 2078-2090, 2013.

31) Cui H, Okamoto Y, Yoshioka K, Du W, Takuwa N, Zhang W, Asano M, Shibamoto T, Takuwa Y. Sphingosine-1-phosphate receptor 2 protects against anaphylactic shock through suppression of endothelial nitric oxide synthase in mice. J Allergy Clin Immunol 132: 1205-1214, 2013.

32) Cui H. Sphingosine-1-phosphate receptor-2 s protective against lipopolysaccharide-induced acute lung injury. J Juzen Med Society 121: 106-118, 2012.

33) Sanchez T, Thangada S, Wu MT, Kontos CD, Wu D, Wu H, Hla T. PTEN as an effector in the signaling of antimigratory G protein-coupled receptor. Proc Natl Acad Sci USA 102: 4312-4317, 2005.